Article ID: 1006-8775(2016) 03-0296-09

ASYMMETRICAL STRUCTURES OF THE TEMPERATURE AND HUMIDITY OF TROPICAL CYCLONES

YANG Tao (杨 涛)[1,2], LEI Xiao-tu (雷小途)[1], TANG Jie (汤 杰)[1]
(1. Shanghai Typhoon Institute and Laboratory of Typhoon Forecast Technique, CMA, Shanghai 200030 China;
2. Shanghai Meteorological Sci-Tech Service Center, Shanghai 200030 China)

Abstract: Based on NCEP/CFSR 0.5° reanalysis data and the best track data from the Japan Tokyo Typhoon Center, composite and comparative analyses demonstrate the asymmetrical structures of the temperature and humidity in tropical cyclones over the Western North Pacific and the South China Sea from 1979 to 2010. The results are shown as follows. (1) With intensifying tropical cyclones, the flow field tends to become gradually more axisymmetric; however, the asymmetry of the specific humidity in the outer regions is more obvious. (2) In general, tropical cyclones have a non-uniform, vertical, "double warm-core" structure. The "warm-cores" in the lower level of weak tropical cyclones and in the higher level of strong tropical cyclones are the stronger of the two. (3) The distribution area of a "warm-core" is enhanced with cyclone intensification and tends to become more axisymmetric. At 200 hPa, the "warm-core" of a weak cyclone has a weak anticyclone in the center, whereas that of a strong cyclone has a weak cyclone in the center. (4) The "wet-core" of a tropical cyclone is primarily located in the lower level (700-850 hPa). With the cyclone's intensification, the intensity of the "wet-core" increases and the scope of the 0.8 g kg^{-1} specific humidity anomaly tends to expand to higher levels. (5) With the cyclone's deepening, the pseudo-equivalent potential temperature at different levels in different regions increases. In addition, the largest warming rates at each intensity level in the different regions occur in the core area, followed in turn by the envelope and outer areas.

Key words: tropical cyclones; asymmetrical structure; warm-core; wet-core; intensity
CLC number: P444 **Document code:** A
doi: 10.16555/j.1006-8775.2016.03.004

1 INTRODUCTION

Tropical cyclones (TCs) with warm-core structures are cyclonic vortices, which can develop rapidly. Earlier studies often simplified TCs as axisymmetric vortices. However, an ideal axisymmetrical structure is rare and difficult to maintain and TCs always appear asymmetric to different degrees. Lack of awareness concerning the mechanisms relating the TCs asymmetric structure and its intensity change often leads to "inadequate warnings" or "over warnings" of wind and rain effects.

The role of the asymmetrical structure and its accompanying "ventilation" effect on the TC track were first recognized by Chen et al.[1]. Numerous studies have discussed the causes of asymmetrical structures and their impact on TC intensity changes. Earlier studies revealed that the asymmetrical structure of TC circulation is primarily related to the planetary vorticity gradient (Peng and Williams [2]; Bender [3]). The average flow through TC circulation also affects the asymmetrical structure of TCs (Bender [3]; Peng et al.[4]). Numerical simulation studies have shown that environmental vertical wind shear could effectively dominate TC structures (DeMaria[5]; Frank and Ritchie[6]; Jones [7]; Frank and Ritchie [8]). Other studies have indicated that the distribution of vapor near the TC circulation could induce asymmetrical structures (Dunion and Velden[9]). Theory analyses and numerical experiments have discussed the effects of diabatic heating on asymmetrical structures in TCs (Lei [10-11]). Recent studies have shown that the asymmetrical structure of clouds and precipitation in TC circulations is gradually gaining more attention (Kossin and Schubert[12]; Kossin et al.[13]; Chen et al.[14]; House[15]), as is research concerning the influence of asymmetrical structures on TCs (Duan et al.[16]; Wang and Wu[17]).

While studies have focused on asymmetrical dynamical structures (Gao and Wang[18]; He et al.[19]; Li et al.[20]), the asymmetry of the humidity is relatively less discussed. Moreover, in previous studies of the asymmetrical structure of TCs, the resolution of the reanalysis has been relatively coarse (Fu et al.[21]; Yuan et al.[22]); however, high-resolution data may be useful to analyze the details of the asymmetrical structure. In recent years, following further studies of the fine structures in the eye area and the inner and outer spiral

Received 2014-10-31; **Revised** 2016-05-12; **Accepted** 2016-07-15
Foundation item: Major State Basic Research Program of China (2013CB430305); National Natural Science Foundation of China (41475060, 41275067, 41305049); Public Benefit Research Foundation of China (GYHY201406010)
Biography: YANG Tao, M.S., primarily undertaking research on tropical cyclones.
Corresponding author: TANG Jie, e-mail: tangj@mail.typhoon.gov.cn

rainbands, more stringent requirements have been put forward for the study of fine asymmetrical structures. Utilizing the newer 0.5° reanalysis data of the Climate Forecast System Reanalysis (CFSR) developed by the National Centers for Environmental Prediction (NCEP) to conduct synthetic analysis of TCs over the Western North Pacific and the South China Sea from 1979 to 2010, we will discuss the asymmetrical structural characteristics of the temperature and humidity for different TC intensities and their possible relation with the TC intensity. Section 2 introduces the datasets and the analysis methods. In Section 3, we analyze the asymmetrical structure of the temperature and humidity for different TC intensity grades. The evolution of the temperature and humidity characteristics in different TC regions will be discussed in Section 4. A short summary is given in Section 5.

2 DATASETS AND METHODOLOGY

The NCEP/CFSR data utilize the atmosphere-ocean-land surface-sea ice coupling system to generate third-generation, high-resolution global reanalysis products (Decker et al.[23]). In contrast to other reanalysis datasets (including JRA-25, JRA-55, ERA-40, ERA-Interim, and MERRA), Murakami observed that in terms of the characterization the spatial and temporal distribution of global TCs, the interannual variability in the TC frequency, lower false alarm rates, and TC structure and strength, JRA-55 and CFSR have better performances [24]. However, because of the coarse resolution of JRA-55 (1.25°), it may not have the potential to demonstrate the fine structures of TCs comparing with the 0.5° resolution of CFSR. Therefore, the CFSR dataset has two virtues for a TC diagnosis, high spatial resolution, and accurate structural analysis capabilities. In addition, synthetic analyses of fine TC structures based on this relatively new high-resolution CFSR dataset have been less studied. This study analyzes the fine asymmetrical structures of different TC intensity grades using CFSR data during the period from 1979 to 2010. The CFSR has a horizontal resolution of 0.5 × 0.5°, 37 vertical layers from 1 to 1 000 hPa, and a 6-h time interval. The TC intensity data used herein is obtained from the Tokyo Typhoon Center best track data.

To classify the TC intensity according to the Chinese Meteorology Agency Standard of TC Grades (GBT, 19201-2006) implemented in June 2006, the TCs records from the Tokyo Typhoon Center best track data were divided into six levels: tropical depression (TD), tropical storm (TS), severe tropical storm (STS), typhoon (TY), severe typhoon (STY), and super typhoon (SPTY). Corresponding to the wind speed interval, the six TC thresholds of the TC intensities were as follows: 10.8–17.1 m·s^{-1}, 17.2–24.4 m·s^{-1}, 24.5–32.6 m·s^{-1}, 32.7–41.4 m·s^{-1}, 41.5–50.9 m·s^{-1}, and ≥ 51.0 m·s^{-1}, respectively. From 1979 to 2010, the numbers of samples of each TC intensity are shown in Table 1. TCs that may be related to landing or extratropical transition were removed.

In this study, TCs of different intensity grades (the samples in Table 1) were synthesized. The synthetic area was in a range of 20 × 20° latitude and longitude from the coordinate origin in the TC center, and the x and y axes represented the zonal and meridional directions, respectively. While calculating the TC circulations, we regarded the TC center as the origin point and selected a circular area with a radius of 5°. According to Wang [25] and Chen et al.[26], and as shown in Fig. 1, we defined the inner core, envelope region, and outer region to represent distances of 50 km from the TC center for the inner core (dark blue), 50-200 km for the envelope (yellow), and the rest of the range for the outer region (light blue).

Table 1. The number of samples on different TC Intensity Grade

Total samples	TD	TS	STS	TY	STY	SPTY
24 465	7 481	5 728	4 419	4 329	1 783	725

3 THE CHARACTERISTICS OF THE TEMPERATURE AND HUMIDITY AT DIFFERENT TC INTENSITIES

3.1 *Asymmetry in the horizontal direction*

Figure 2 shows the flow field and the specific humidity fields at 925 hPa according to the different TC intensity grades (TD, TS, STS, TY, STY, and SPTY). In Fig.2a, the flow fields show an obvious "concentrated east and sparse west" asymmetrical structure. The specific humidity within the TC circulation is also significantly higher than that in the environmental field (approximately 2 g·kg^{-1}) and closer to the TC center, indicating higher specific humidity, similar to previous results (Zhou et al.[27]). When the intensity increases to the TS level, the flow field in the west becomes slightly more dense so that the asymmetry of the flow field weakens. The specific humidity within the circulation is significantly higher than in the TD level and the maximum of the specific humidity near the TC center can be up to 16.88 g·kg^{-1} (Fig.2b). With the intensity level rising, the flow field tends to become more symmetric and the specific humidity in the circulation increases (the maximum specific humidity near the TC center can be up to 18.78

$g \cdot kg^{-1}$ and its difference from the environmental field reaches 3.5 $g \cdot kg^{-1}$) (Figs.2c-2f).

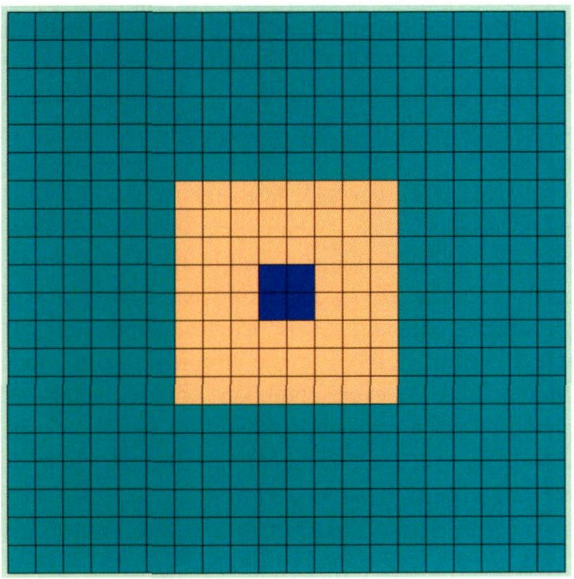

Figure 1. The distribution of different TC areas (inner core, envelope, outer).

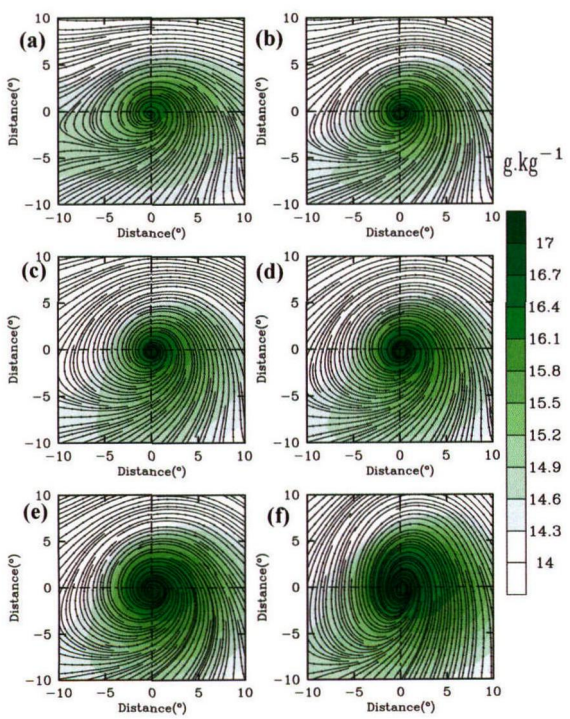

Figure 2. The horizontal distribution of flow field (solid line) and specific humidity fields (shaded area) at 925hPa on different TC intensity (unit: $g \cdot kg^{-1}$) (a-f respectively stands for TD, TS, STS, TY, STY, SPTY). TC center is located at (0, 0) origin, and negative values and positive values of x axis stand for west and east respectively, and negative values and positive values of y axis stand for south and north respectively. The grid spacing of latitude and longitude is 1°.

To present the asymmetry of the specific humidity, the specific humidity of different intensity TCs at 925 hPa were Fourier decomposed (Fig.3). Using the synthesis in the TC center as the center point, with 5° latitude as the radius of the circular area, the average values and the maximum asymmetrical component of the low wavenumber in the TC circulation was obtained (Table 2). Combining Fig.3 and Table 2, we observe that the wavenumber-1 asymmetrical component in the inner core is stably maintained at ±0.2 $g \cdot kg^{-1}$ with increasing intensity, which shows that the symmetry is high in the inner core. In the envelope area, the wavenumber-1 asymmetrical component is increasing; therefore, the asymmetry in the envelope is intensifying. According to Table 2, the maximum of the wavenumber-1 asymmetrical component increases from 0.48 $g \cdot kg^{-1}$ to 1.68 $g \cdot kg^{-1}$ and then decreases to 0.98 $g \cdot kg^{-1}$, which indicates that the asymmetry in the outer region is generally enhanced when the TC intensity increases. In addition, the order and range of the wavenumber-2 and wavenumber-3 asymmetrical components are small, so that they will not repeat.

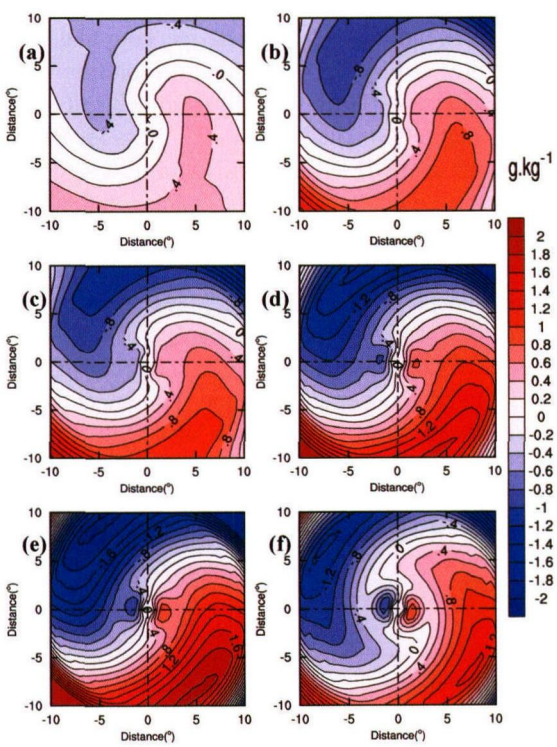

Figure 3. Same as Fig.2 but for the wavenumber-one asymmetrical distribution of 925hPa specific humidity fields (shaded area) on different intensity (unit: $g \cdot kg^{-1}$).

In general, the "warm-cores" of the TCs are always located at the level of 200 hPa. Regarding the differences in the "warm-cores" for each TC intensity grade in Fig.4, we see that the maximum temperature anomalies in the TD center are approximately 0.7 K and the range of values greater than 0.6 K is quite small. The range of the "warm heart" in TS expands rapidly, and the high pressure center tends to increase and move eastward (Fig.4b). With increasing intensity, the "warm-core" expands and gradually evolves into a more

Table 2. The contrast of low wavenumber asymmetrical component of the 925hPa specific humidity fields on different TC intensity (unit: $g \cdot kg^{-1}$).

	TD	TS	STS	TY	STY	SPTY
Average	15.41	15.32	15.46	15.52	15.54	16.37
The maximum of wavenumber-1 asymmetry	0.48	0.89	0.97	1.24	1.68	0.98
The maximum of wavenumber-2 asymmetry	0.19	0.23	0.15	0.24	0.37	0.34
The maximum of wavenumber-3 asymmetry	0.07	0.06	0.04	0.12	0.11	0.16

regular round shape. The "warm-core" gradually evolves into a low pressure center and tends to coincide with the warm center. The maximum temperature anomaly in the SPTY center is approximately 3.7 K (Figs.4c-4f).

In other levels of the troposphere (300 hPa, 500 hPa, and 850 hPa), the temperature anomalies (warm-core) of the different intensity grades are similar to that shown in Fig.4. The range of the "warm heart" (positive temperature anomalies) is relatively small and shrinks with decreasing height. This agrees with previous studies of the asymmetrical structure and "warm-core" structure conducted by Chen and Ding[28] and Halverson et al.[29].

3.2 *Non-uniform structures in the vertical direction*

The development of TCs is inseparable from the abundant moisture conditions in the middle and lower level troposphere (Chen et al.[26] and Gray[30]). Fig.5 shows a meridional vertical section of the specific humidity anomalies for different TC intensity grades. All the intensity TC grades are observed to possess an obvious "wet-core" (a maximum positive anomaly) at the 850-hPa level. In Fig.5a, combined with Table 3, the "wet-core" is seen to be primarily located from 850 to 700 hPa and the intensity of the "wet-core" reaches 0.88 $g \cdot kg^{-1}$. Fig. 5b shows that the intensity of the "wet-core" has already intensified to 0.98 $g \cdot kg^{-1}$ at the TS level. With increasing TC intensity levels, the strength of the "wet-core" also increases, and the 0.8 $g \cdot kg^{-1}$ range of the specific humidity anomalies continues to extend to high layers from 650 to 550 hPa (Figs. 5c-5f).

Table 3. The intensity of the "wet-core" and the extended level of specific humidity on different intensity.

	TD	TS	STS	TY	STY	SPTY
The intensity of the wet-core ($g \cdot kg^{-1}$)	0.88	0.98	1.08	1.24	1.38	1.42
The maximum extended level of 0.8$g \cdot kg^{-1}$(hPa)	650	650	650	600	550	550
The maximum extended level of 1.0$g \cdot kg^{-1}$(hPa)	/	/	775	650	600	600

Figure 6 shows the meridional vertical section of the temperature anomalies for the different intensity grades. As seen in Fig.6a, TD shows a "double warm-core" (two maximum positive anomalies) structure, which are located at 300 hPa (warm-core in the high level) and 800 hPa at a height of approximately 2 km (warm-core in the low layer). When the TC intensity increases, the strength of the "warm-core" in the high and low layers both increases. Note that the "warm-cores" in the high and low layers evolve gradually from an irregular shape to an oval and the range of the "warm-cores" shrink (Fig.6). Combining Fig.6 and Table 4, we see that the "double warm-core" structure with high and low levels is prevalent at each TC intensity level. In weak TCs (TD, TS, and STS), the high-level "warm-core" is weaker than the low-level "warm heart," whereas in severe TCs (TY, STY, and SPTY), the high-level "warm-core" is stronger than the low-level "warm heart".

3.3 *Vertical distribution of vapor for different intensity grades*

Vapor transport and latent heat release are closely related to the "warm-cores" and "wet-cores" of the TCs. In Fig.7a, the moisture fluxes of the maximum positive anomaly areas are located north of the TC center from 925 hPa to 850 hPa and its maximum value is 2.0×10^{-2} $g \cdot s^{-1} \cdot hPa^{-1} \cdot cm^{-1}$. The large positive anomalies of the moisture fluxes greater than 1.0×10^{-2} $g \cdot s^{-1} \cdot hPa^{-1} \cdot cm^{-1}$ extend to the 600-hPa layer (Fig.7a), while negative anomalies exist near the TC center, which may imply environmental vapor transport to the TC circulation. The vertical gradient of positive vapor flux anomalies increases rapidly in TS and the center values reach 4.8×10^{-2} $g \cdot s^{-1} \cdot hPa^{-1} \cdot cm^{-1}$ (Fig.7b). As in Fig.7f, the maximum positive moisture flux anomalies reach 14.1×10^{-2} $g \cdot s^{-1} \cdot hPa^{-1} \cdot cm^{-1}$ and their range extends from the nearby surface to 800 hPa. The range of positive moisture flux anomalies greater than 1.0×10^{-2} $g \cdot s^{-1} \cdot hPa^{-1} \cdot cm^{-1}$ extends to the 350-hPa layer in the vertical direction and approximately 7° latitude in the horizontal direction. This results in abundant moisture for the TCs. It is interesting that the maximum positive moisture flux anomaly is gradually intensifying, its range is expanding, and the vertical gradient is increasing with

Table 4. The intensity of the high and low layer "warm-core" on different TC intensity (Unit: K)

	TD	TS	STS	TY	STY	SPTY
Warm-core (high)	0.58	0.76	0.94	1.19	1.29	1.37
Warm-core (low)	0.71	1.04	1.26	1.14	1.01	1.01

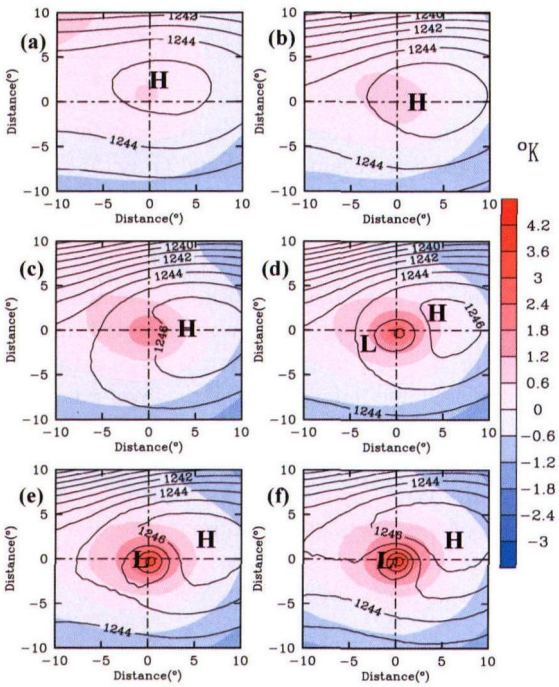

Figure 4. The horizontal distribution of height field (solid line) and temperature field (shaded area) at 200 hPa on different intensity (unit:K).

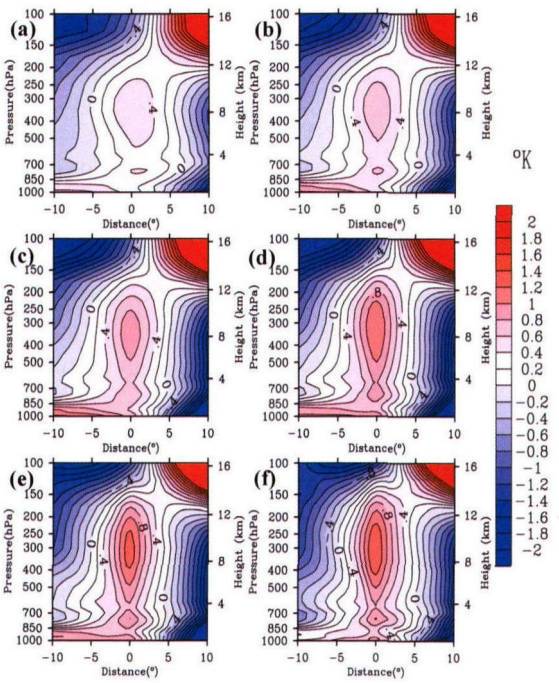

Figure 6. Same as Fig.5 but for the anomaly temperature on the meridional vertical section (Unit: K).

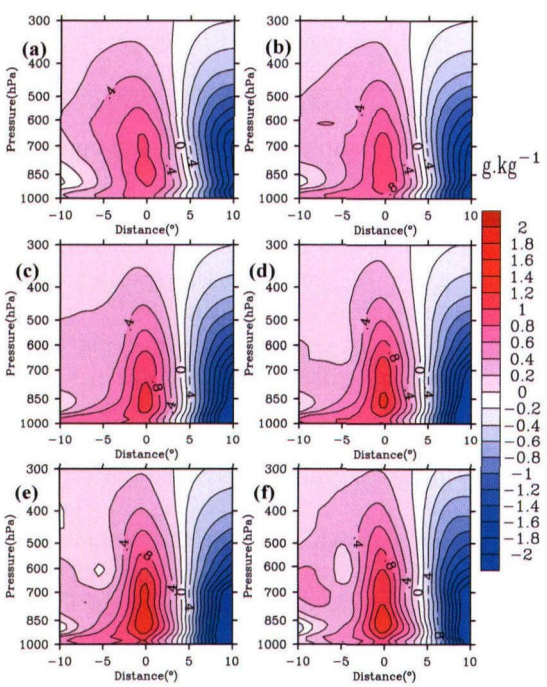

Figure 5. The meridional vertical section of the anomaly specific humidity on different intensity (Unit: g·kg^{-1}) (a-f represent the TC intensity TD, TS, STS, TY, STY, SPTY). TC center is located at 0, and negative values and positive values of x axis stand for south and north respectively. The grid spacing of latitude and longitude is 1°.

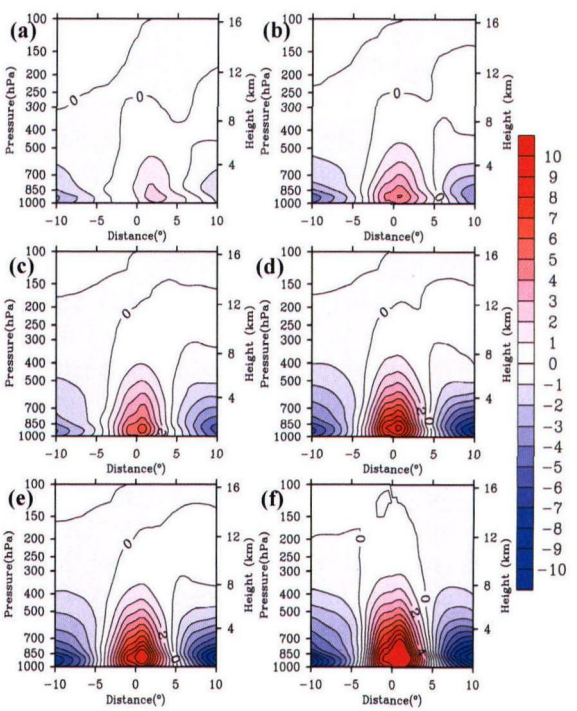

Figure 7. Same as Fig.5 but for the anomaly vapor fluxes (Unit : 10^{-2}g·s^{-1}·hPa^{-1}·cm^{-1}).

growing TC intensity, which is favorable to the presence of a stronger "wet-core".

Figure 8a shows that the moisture convergence is generally concentrated from the surface layer to 850 hPa and that the maximum convergence is approximately 12.9 $\times 10^{-7}$ g $\cdot s^{-1}$ hPa^{-1} cm^{-2}, which is consistent with the vapor concentration in Fig.7a. However, this convergence does not generate an effective moisture divergence and may not establish an effective vapor pumping system in the TD stage. In the TS stage, the maximum convergence reaches 19.1 $\times 10^{-7}$ $g \cdot s^{-1} \cdot hPa^{-1} \cdot cm^{-2}$ in the lower level and a corresponding vapor divergence in the higher level from 500 to 400 hPa is obvious. This means that the TS stage may have established a relatively comprehensive vertical vapor transporting mechanism, whereby a large amount of vapor is transported through the low-level convergence to the high levels. Then, high-level cumulus release large amounts of latent heat, supporting the stronger "warm-core" (Fig.8b) and forming a positive feedback mechanism, which is continuously enhanced. With increasing TC intensity, the configuration of the convergence and divergence is more perfect and the vapor pumping is more effective, favoring the formation of a "warm-core".

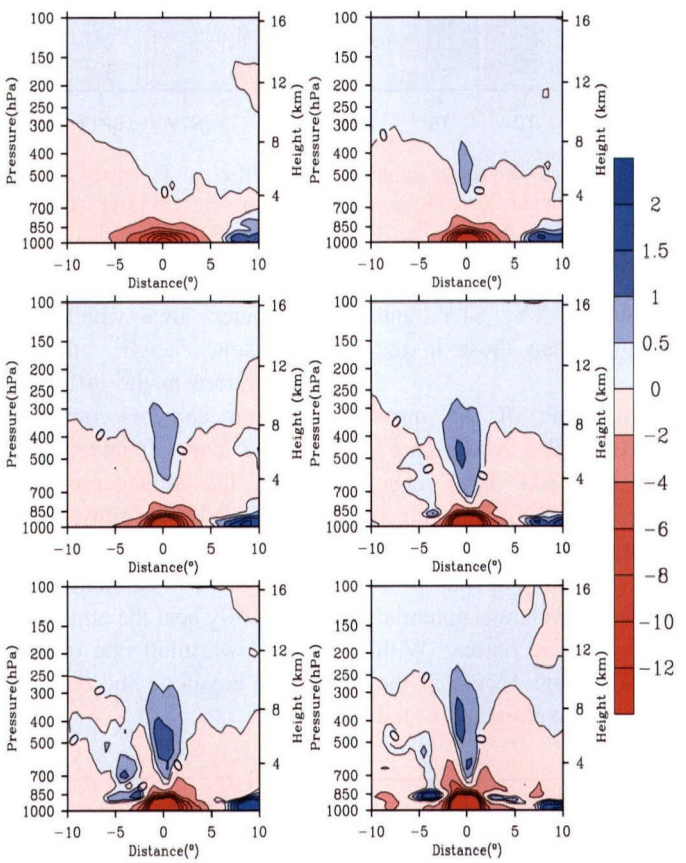

Figure 8. Same as Fig.5 but for the divergence of vapor fluxes (Unit : $10^{-7} g \cdot s^{-1}$ $hPa^{-1} \cdot cm^{-2}$).

4 HORIZONTAL DISTRIBUTION OF THE TEMPERATURE AND HUMIDITY STRUCTURE WITH HEIGHT AND INTENSITY

Figure 9 shows the vertical distribution of the vapor fluxes in different regions for different intensity grades. In TDs, vapor fluxes in the inner core, envelope area, and outer region rapidly increase with decreasing height. When the TC is in the TS stage, the vertical gradients of the vapor fluxes in all regions are significantly higher than those in the TD stage. Note that the inner core is drier than the outer region in the TD stage and vapor in the inner core is more sufficient than in the outer region in the TS stage, which is called the "overtaking phenomenon" that the value of the vapor in the inner core is higher than that in the outer region. A possible reason for this is that TDs do not establish effective pumping systems and may not efficiently transport moisture to the upper levels via the Conditional Instability of the Second Kind (CISK) mechanism. Therefore, the development of TDs primarily depends on the vapor supply from the environmental field. Meanwhile, stronger TSs establish a comprehensive pumping system and primarily extract vapor from the warm ocean to the upper levels via the CISK mechanism. In addition, accompanying the increasing intensity, the vapor fluxes of different TC grades show a rapid increasing trend in different regions and at different heights. In particular, the vertical

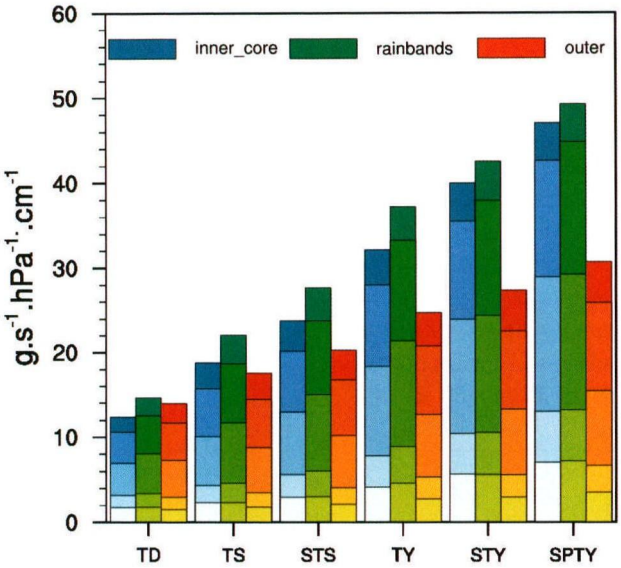

Figure 9. The distribution of the vapor fluxes on various height levels of different TC intensity in different regions (unit: $10^{-2}g \cdot s^{-1} hPa^{-1} \cdot cm^{-1}$), where the blue colors represent inner core, the green colors represent envelope area, the red colors represent outer, every histogram dividing solid line represents 400hPa, 500hPa, 700hPa, 850hPa, 925hPa levels of vapor fluxes from the bottom-up.

gradients of the vapor fluxes in the TY, STY, and SPTY stages are remarkably higher than those in the TD or TS stages.

Chen et al. [26] indicated that one of the most important structural features of TCs is the "warm-core" structure in the high level (200-300 hPa). The pseudo-equivalent potential temperature in the inner core is higher than the surrounding atmosphere by 10-15 K in the upper troposphere. In Fig.10a, with increasing height, the pseudo-equivalent potential temperature in the different regions decreases. With intensifying TC, the largest warming rate occurs in the inner core region, followed by the envelope area and the outer area which has minimum heating. With increasing height, the pseudo-equivalent potential temperature in the different regions increases (Fig.10b). Here, it can be concluded that internal atmosphere heating can effectively increase the temperature and reduce the surface pressure because the inner core has high inertial stability. Conversely, the envelope area with its inertial instability transfers the atmo spheric heating to gravitational oscillations and cannot effectively heat the atmosphere (Gray[31] and Wang[32]). The largest warming rate occurs in the inner core, followed by the envelope and the outer region in turn.

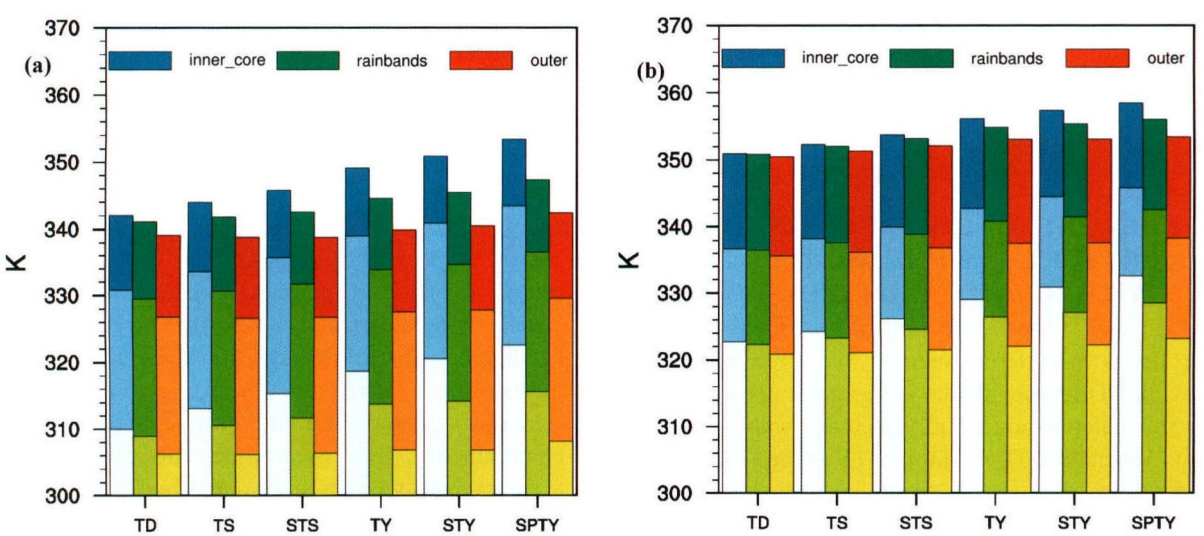

Figure 10. The distribution of the pseudo-equivalent potential temperature on various height levels of different TC intensity in different regions (unit: K), where the blue colors represent inner core, the green colors represent envelope area, the red colors represent outer. (a) every histogram dividing solid line represents 700hPa, 850hPa, 925hPa from the bottom-up (b)every histogram dividing solid line represents 400hPa, 300hPa, 200hPa from the bottom-up.

5 CONCLUDING REMARKS

High-resolution NCEP/CFSR datasets were used to study the asymmetrical structures of the temperature and humidity at different TC intensities over the Western North Pacific and the South China Sea from 1979 to 2010 in this study. The evolution of the structural characteristics in different life stages was revealed and may help improve our understanding of the structural evolu tion and its role in the TC intensity. The results are as follows.

(1) As tropical cyclones intensify, the asymmetry of the flow field tends to become gradually more axisymmetric. The humidity asymmetry in the envelope area and the outer region is enhanced, while the inner core has high symmetry with increasing intensity.

(2) In general, TCs have non-uniform vertical structures of the so called "double warm-core." The "warm-cores" in the lower level of weak tropical cyclones are stronger than those in the higher-level, whereas severe tropical cyclones show the opposite trend.

(3) The horizontal area and axisymmetry of the "warm-core" increases with tropical cyclone intensifica tion. In addition, at 200 hPa, the "warm-cores" in the weak cyclones have a weak anticyclone in their centers, whereas those of strong cyclones have cyclonic motion in their centers.

(4) The "wet-core" of a tropical cyclone can be observed at a level of approximately 700-850 hPa. With increasing cyclone intensity, the intensity of the "wet-core" increases and the core area, with a threshold of >0.8 $g \cdot kg^{-1}$, tends to expand to higher levels.

(5) With increasing cyclone intensity, the pseudo-equivalent potential temperature at different levels in different regions of the cyclones increases. In addition, the largest heating rates of each intensity level in different regions always occur in the core region, followed by the envelope and outer regions.

Note that the data resolution used in this study is still relatively low. In addition, the difference between the selection of the TC intensity data and the criteria for TC classification could lead to an analysis bias. Based on the structural features such as the "double warm heart," the "wet-core" revealed by the statistics, and its relation with the intensity, these results still require further study based on higher resolution reanalysis data and observations.

REFERENCES:

[1] CHEN Lian-shou, XU Xiang-de, XIE Yi-yang, et al. Effects of Typhoon abnormal movement and the asymmetrical structure of thermodynamic instability in its outer area [J]. Atmos Sci, 1997, 21(1): 83-90.

[2] PENG M S, WILLIAMS R T. Dynamics of vortex asymmetries and their influence on vortex mo tion on a beta plane [J]. J Atmos Sci, 1990, 47(16): 1 987-2 003.

[3] BENDER M A. The effect of relative flow on the asymmetric structure in the interior of hurricanes [J]. J Atmos Sci, 1997, 54(6): 703-724.

[4] PENG M S, JENG B F, WILLIAMS R T. A numerical study on tropical cyclone intensification Part I: Beta effect and mean flow effect [J]. J Atmos Sci, 1999, 56 (10): 1 404-1 423.

[5] DEMARIA M. The effect of vertical wind shear on tropical cyclone intensity change [J]. J Atmos Sci, 1996: 53(14): 2 076-2 087.

[6] FRANK W M, RITCHIE E A. Effects of environmental flow upon tropical cyclone structure [J]. Mon Wea Rev, 1999, 127(9): 2 044-2 061.

[7] JONES S C. On the ability of dry tropical-cyclone-like vortices to withstand vertical shear [J]. J Atmos Sci, 2004, 61(1): 114-119.

[8] FRANK W M, RITCHIE E A. Effects of environmental flow on the intensity and structure of numeri cally simulated hurricanes [J]. Mon Wea Rev, 2001, 129 (9): 2 249-2 269.

[9] DUNION J P, VELDEN C S. The impact of the Sahara air layer on Atlantic tropical cyclone activity [J]. Bull Amer Meteor Soc, 2004, 85(3): 353-365.

[10] LEI Xiao-tu. The numerical experiments about the influences of diabatic role on TCs structure [J]. J Trop Meteorol, 1998, 14(3): 208-216.

[11] LEI Xiao-tu. The influences of diabatic on the non-uniform structure of TCs in radial [J]. J Marine, 2000, 22(4): 26-30.

[12] KOSSIN J P, SCHUBERT W H. Mesovortices, polygonal flow patterns, and rapid pressure falls in hurricane-like vortices [J]. J Atmos Sci, 2001, 58(15): 2 196-2 209.

[13] KOSSIN J P, MCNOLDY B D, SCHUBERT W H. Vortical swirls in hurricane eye clouds [J]. Mon Wea Rev, 2002, 130(12): 3 144-3 149.

[14] CHEN S S, KNAFF J A, MARKS F D. Effects of vertical wind shear and storm motion on tropical cyclone rainfall asymmetries deduced from TRMM [J]. Mon Wea Rev, 2006, 134(11): 3 190-3 208.

[15] HOUZE R A. Clouds in tropical cyclones [J]. Mon Wea Rev, 2010, 138(2): 293-344.

[16] DUAN Yi-hong, YU Hui, WU Rong-sheng. The current study about tropical cyclone intensity [J]. J Meteorol, 2005, 63(5): 638-642.

[17] WANG Y Q, WU C C. Current understanding of tropical cyclone structure and intensity changes-a review [J]. Meteorol Atmos Phys, 2004, 87(4): 257-278.

[18] GAO Fan, WANG Hong-qing. Numerical Simulation and the analysis of Structural Evolution Characteristics on typhoon Matsa (0509) [J]. J Beijing Univ, 2008, 44(3): 385-390.

[19] HE Hui-qing, WANG Zhen-hui, JIN Zheng-run. The effects of asymmetrical circulation on tropical cyclone intensity [J]. J Meteorol, 2008, 24(3): 249-253.

[20] LI Jiang-nan, WU Guo-qiang, WANG Gang et al. The numerical simulation Vongfong (2002) on the inner core structure before and after landfall and rapid intensification offshore [J]. J Meteorol, 2008, 24 (5): 441-448.

[21] FU Ju, DONG Zhen-hua, TAN Ji-qing. The study of typhoon warm-core before and after landfalling [J]. Bul Tech, 2011, 27(1): 18-24.

[22] YUAN Jin-nan, ZHOU Wen, HUANG Hui-jun, et al. The observational analysis on asymmetrical distribution of convection about landfalling tropical cyclone "Pearl" and "Prapiroon" in South China [J]. J Meteorol, 2009, 25(4): 385-392.
[23] DECKER M, BRUNKE M A, WANG Z et al. Evaluation of the Reanalysis Products from GSFC, NCEP, and ECMWF Using flux tower observations [J]. J Climate, 2012, 25(6): 1 916-1 944.
[24] MURAKAMI H. Tropical cyclones in reanalysis data sets [J]. Geophys Res Lett, 2014, 41(3): 1-9.
[25] WANG Y Q. How do outer spiral rainbands affect tropical cyclone structure and intensity?[J]. J Atmos Sci, 2009, 66(5): 1 250-1 273.
[26] CHEN Lian-shou, DUAN Yi-hong, SONG Li-li et al. The forecasting and disaster of typhoon [M]. Beijing: China Meteorology Press, 2012, 8-19.
[27] ZHOU Ling-li, ZHAI Guo-qing, WANG Dong-hai et al. Mesoscale numerical study of typhoon storm and asymmetrical structure analysis about "Weipa" (0713) [J]. Meteorol Sci, 2011, 35(6): 1 047-1 051.
[28] CHEN Lian-shou, DING Yi-hui. The introduction to Western Pacific typhoon [M]. Beijing: Science Press, 1979, 31-64.
[29] HALVERSON J B, SIMPSON J, HEYMSFIELD G et al. Warm core structure of Hurricane Erin diagnosed from high altitude dropsondes during CAMEX-4 [J]. J Atmos Sci, 2006, 63(1): 309-324.
[30] GRAY M W. Global view of the origin of tropical disturbances and storms [J]. Mon Wea Rev, 1968, 96 (10): 669-700.
[31] HACK J, SCHUBERT W H. Nonlinear response of atmospheric vortices to heating by organized cumulus convection [J]. J Atmos Sci, 1986, 43(15): 1 559-1 573.
[32] WANG Y Q. Structure and formation of an annular hurricane simulated in a fully compressible, nonhydrostatic model-TCM4 [J]. J Atmos Sci, 2008, 65 (5): 1 505-1 527.

Citation: YANG Tao, LEI Xiao-tu and TANG Jie. Asymmetrical structures of the temperature and humidity of tropical cyclones [J]. J Trop Meteorol, 2016, 22(3): 296-304.